Supercritical Expansion Flow in Rouse Modified and Reversed Transitions

By Somendra K. Mazumder,[1] and Willi H. Hager,[2] Member, ASCE

Abstract: Supercritical expansion flow in nearly horizontal rectangular channels is actually based on the Rouse wall geometry. As the transition structure becomes extremely long, a revised design involving significant shortening is presented. The revised design is based on separate observations of the flow in the abrupt expansion, and two alternative designs, i.e. the modified and the reversed Rouse wall curves. The modified Rouse wall curve is found to give no improvement over the abrupt expansion and is thus dropped. The reversed Rouse wall curve yields better flow conditions than the abrupt expansion and is significantly shorter than the original Rouse curve. The semiempirical approach accounts for the effects of streamline curvature and viscosity. The free surface is shown to be governed by the Froude similarity law; the velocity field involves significant Reynolds effects in addition. Thus, the latter may not be analyzed by a generalized approach. The surface of flow may further be analyzed when using a correctly distorted coordinate system. Thus, insight is given in the surface profiles along the expansion axis and the side wall. Design recommendations based on the reversed Rouse wall curve end the paper.

Introduction

Supercritical channel flow is prone to perturbations as shock or cross waves are generated. The height of the standing wave is directly proportional to the approach Froude number (Hager 1992). In spillway chutes with large Froude numbers, shock waves are thus a major concern.

Perturbations as typically encountered in chutes include bends, contractions, junctions, or expansions. The last is studied in the present paper. Chute expansions may occur in portions of flat slope following a steeper reach, or when discharge is added. Also, expansion-type flow occurs in combining structures in front of stilling basins when a single chute channel is working and where the flow is allowed to expand transversely.

In a previous study (Hager and Mazumder 1992), abrupt expansion was analyzed by a semiempirical approach. It was found that the free surface satisfies similarity according to Froude's law provided that the minimum flow depth is not to small to involve Reynolds effects. For such flow, the flow depths may be scaled by the approach flow depth h_0: the length scale is $b_0 F_0$, with b_0 = approach width; $F_0 = V_0(gh_0)^{-1/2}$ = approach Froude number; and g = gravitational acceleration. Of particular design relevance in Hager and Mazumder (1992) is the maximum wall flow depth $h_{wM}/h_0 = 0.81$ at location $x_M/(b_0F_0) = 1.33$, for an expansion ratio $\beta = b_2/b_0 = 3$, with b_2 as tailwater width of the rectangular chute. For $\beta = 2$ and 5 the corresponding values are $h_{wM}/h_0 = 0.96$ and 0.67 at locations $x_M/(b_0F_0) = 0.94$ and 2.08, respectively. Note that the origin of coordinate system (x, y) is at the centerline of the expansion section.

---

[1]Prof. of Civ. Engrg., Delhi Coll. of Engrg., Delhi 110 006, India.

[2]Sr. Res. Engr., Swiss Federal Inst. of Tech., Versuchsanstalt für Wasserbau, Hydrologie und Glaziologie (VAW), ETH-Zentrum, CH-8092 Zurich, Switzerland.

Note. Discussion open until July 1, 1993. To extend the closing date one month, a written request must be filed with the ASCE Manager of Journals. The manuscript for this paper was submitted for review and possible publication on April 27, 1992. This paper is part of the ***Journal of Hydraulic Engineering***, Vol. 119, No. 2, February, 1993. ©ASCE, ISSN 0733-9429/93/0002-0201/$1.00 + $.15 per page. Paper No. 3879.

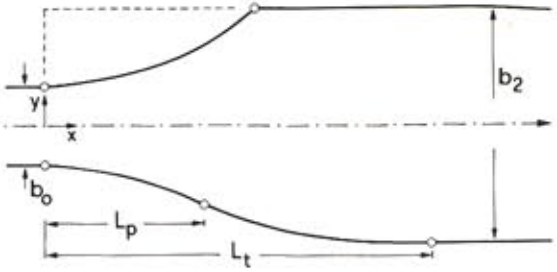

FIG. 1. Wall Geometry for Modified (Top) and Reversed (Bottom) Rouse Wall Curves

The purpose of the present paper is to determine whether the wall height could be reduced when a gradually curved wall geometry instead of the abrupt expansion is used. Rouse et al. (1951) forwarded a design involving the modified wall curve for the front portion and a reversed curve for the back portion (Fig. 1). The so-called Rouse expansion corresponds to an S-shaped wall curve with its center of curvature outside the flow in the front portion, a point of inflexion, a second portion with its center of curvature inside the flow (Appendix I). The length L_t/b_0 of the transition curve depends linearly on the approach Froude number F_0 and the expansion ratio β. As an example, it becomes $L_t/(b_0F_0) = 7.5$ for $\beta = 3$—that is, $L_t/b_0 = 37.5$ for $F_0 = 5$ or even $L_t/b_0 = 75$ for $F_0 = 10$. This transition length is significant, and methods of reduction should be sought, enabling the design of economic structures.

Experimental Installation

The experiments were conducted in a 10-m-long rectangular, horizontal channel. The water was pumped into a 2 m × 2 m steel tank of 3 m height, where porous walls were inserted to improve the uniformity of the outflow. The tank outlet was streamlined by bottom and side polyvinyl chloride (PVC) elements. The height of outflow could be varied with a gate on which a 5°-sloping, 0.40-m-long cover was attached. The rectangular jet of $b_0 = 0.50$ m width and variable height was discharged into the approach channel of 1.2 m length.

At $x = 0$, the approach channel widened abruptly to $b_2 = 1.5$ m. The bottom and the right-hand side wall were of black PVC, and the left-hand side wall was of glass, allowing visual observation. The abruptly expanding channel was used to establish the flow conditions in a basic channel configuration (Hager and Mazumder 1992).

The observations with the Rouse wall expansions were also conducted in this channel, by inserting PVC wall elements. In all experiments, the expansion ratio was $\beta = b_2/b_0 = 3$. The Rouse wall curves are defined with the design Froude number F_D, as explained by Chow (1959). The two design Froude numbers $F_D = 4$ and $F_D = 1$ based on the Rouse modified and reversed wall geometries (Appendix I) are considered. In total, four expansion geometries were tested.

The approach flow depths were $h_0 = 48$ mm and 96 mm, as for the abrupt expansion. The maximum discharge was $Q = 270$ L·s^{-1}. Table 1 summarizes the test program with detailed runs, in which both the velocity and

TABLE 1. Test Program of Detailed Runs

Number (1)	Run (2)	F_D (3)	F_0 (4)	h_0 (mm) (5)	Remarks (6)
1	8	4	4	96	Modified
2	9	4	4	96	Reversed
3	24	1	4	48	Modified
4	25	1	8	48	Modified
5	26	1	6	48	Modified
6	27	1	2	48	Modified
7	41	1	4	96	Modified
8	42	1	2	96	Modified
9	43	1	4	96	Reversed
10	44	1	2	96	Reversed
11	45	1	1	96	Reversed
12	48	1	4	48	Reversed
13	49	1	6	48	Reversed
14	50	1	8	48	Reversed

the flow depth fields were established. Additional tests were also run in which the axial and wall profiles only were studied. In Table 1, F_0 refers to the test approach Froude number for a expansion geometry designed for a particular design Froude number $F_D \leq F_0$.

In the detailed experiments, both flow depths h and velocities V were recorded. The flow depths were taken with a conventional point gage (±0.5 mm reading accuracy) extended by an electrical probe indication for free-surface touching. This is important because the usual flow depths were between 10 mm and 60 mm, say, and the local Froude numbers $F = V(gh)^{-1/2}$ thus significantly depend on exact gauging.

The local velocity V was found to vary only slightly in the vertical direction, except for the boundary layer. Thus, a representative velocity magnitude at half of the local flow depth was taken with a miniature current meter of external diameter 10 mm. Also, the local streamline direction was measured with an angle probe. The two-dimensional (2D) velocity field is thus defined. The velocity probe is protected by a cylindrical casing, on the top of which a moveable PVC element was fixed to inhibit air entrainment to the propeller. Extended preliminary observations indicated reliable results for flow depths down to 15 mm and velocities up to 5 m·s^{-1}.

The experimental grid was $\Delta x = 0.2$ m in the streamwise and $\Delta y = 0.05$ m in the transverse directions for the abrupt expansion; Δy was kept equal for the Rouse expansions, but Δx was normally 1 m. This modification was introduced both to save time (the present experimental study includes thousands of observations) and to account for the more uniform flow pattern, for which a dense grid was not necessary.

Flow Characteristics

Modified Rouse Curve

Fig. 2 shows a plot for run 8 in successive reaches, e.g. a modified Rouse curve with design Froude number $F_D = 4$ for an equal approach Froude number $F_0 = 4$, for which the main features of flow are retained. On the upper portion of Fig. 2 contour lines h/h_0 for flow depth are plotted as a

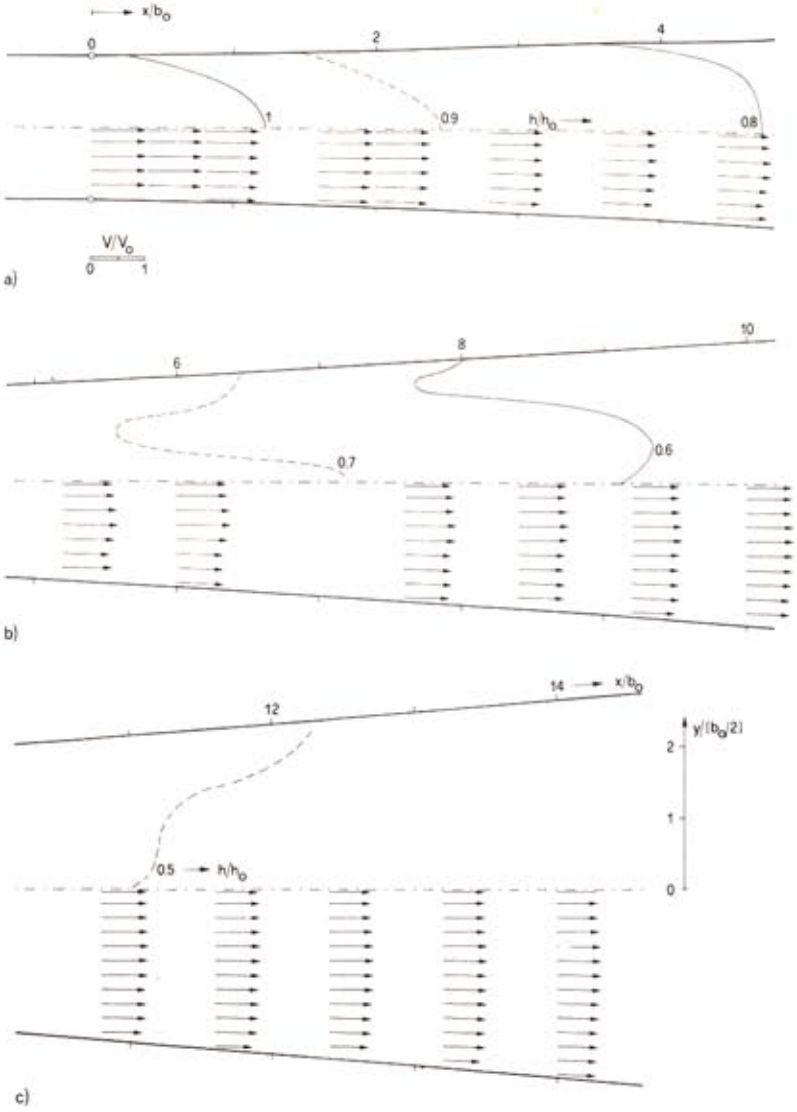

FIG. 2. Modified Rouse Wall Curve Designed for $F_D = 4$, Free Surface Contour Lines h/h_0 (Upper Portion), and Velocity Field V/V_0 (Lower Portion) for $h_0 = 48$ mm, $F_0 = 4$

function of nondimensional position x/b_0 and $y/(b_0/2)$; the 2D velocity field V/V_0 is shown in the lower portion. The scale is not distorted, and one may note only a slight variation of both free-surface and velocity gradients compared to an abrupt expansion (Hager and Mazumder 1992). Because the transition structure is with $L_t/b_0 = 16$ long, significant cost savings result by shortening it.

Fig. 3 shows the flow characteristics for the Rouse modified wall curve

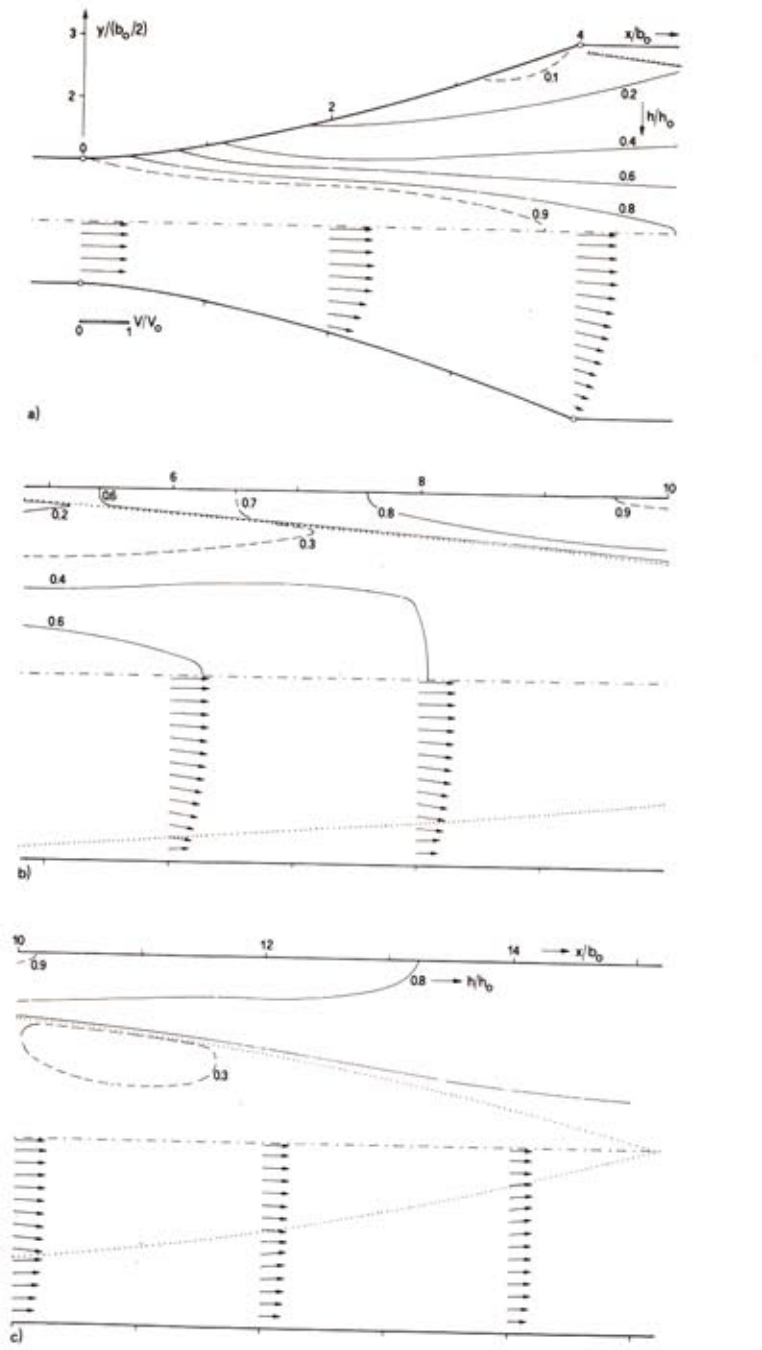

FIG. 3. Modified Rouse Wall Curve for $F_D = 1$, Free Surface Contours h/h_0 (Upper Portion), and Velocity Field (Lower Portion) for $h_0 = 48$ mm, $F_0 = 8$ (.... = Shock Front)

with a design Froude number $F_D = 1$ for an approach Froude number $F_0 = 8$ (run 25). As expected, this geometry yields an overforced flow, because the actual Froude number is much larger than the design Froude number F_D. The flow uniformity is weak in the expanding portion and gets even worse in the downstream prismatic portion.

Fig. 4 shows photographs corresponding to Figs. 2 and 3. No shocks are observed in the expanding portion of the long transition (they occur in the tailwater channel), but large perturbations form in the short transition, mainly downstream from the transition end.

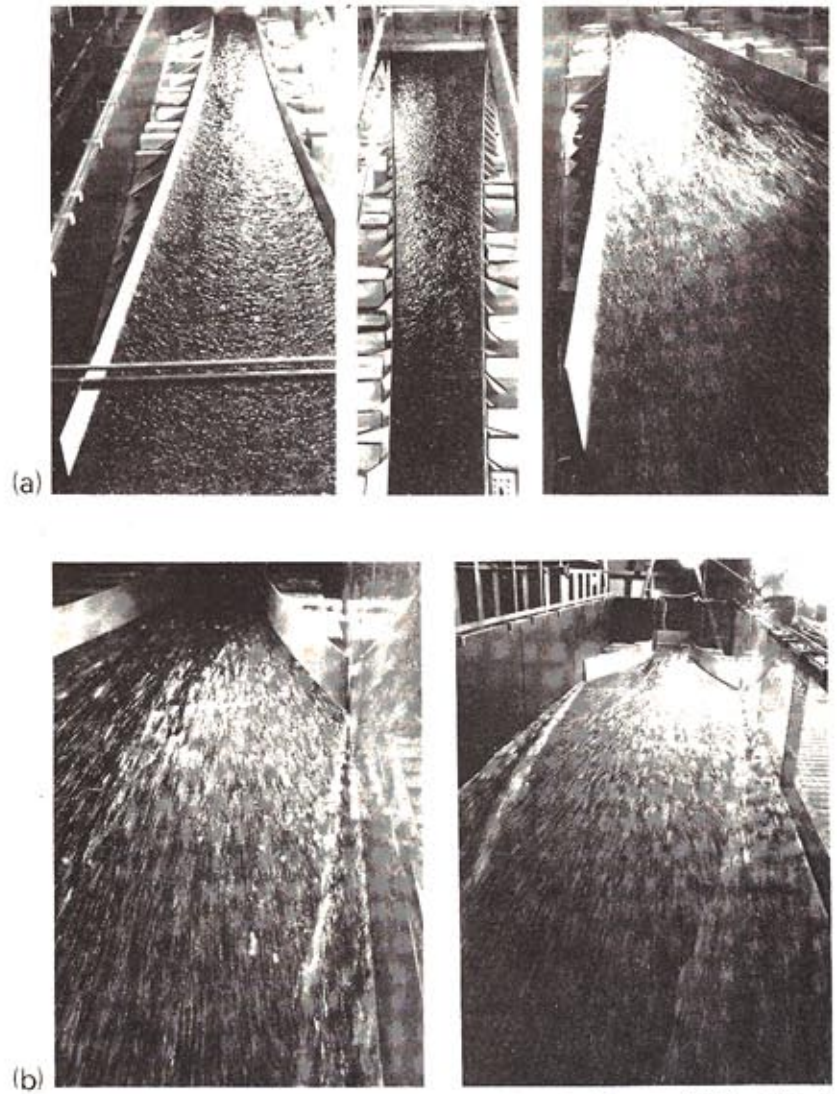

FIG. 4. Rouse Modified Wall Curves, Tailwater Views Relating to: (*a*) Fig. 2 (Top), and (*b*) Fig. 3 (Bottom)

In the next step, the Froude number was reduced to $F_0 = 4$ in the transition designed for $F_D = 1$. Approximately the same pattern of flow as for $F_0 = 8$ resulted, indicating that further reduction in the ratio F_0/F_D is needed for acceptable flow. When F_0/F_D was lowered to 2, definite improvement occurred, as discussed subsequently.

Reversed Rouse Curve

The reversed Rouse wall curve involving smooth curvature changes throughout the transition length is approximately 100% longer than the modified Rouse wall curve. The abrupt change of direction at the latter's end is thus inhibited (Fig. 1). Rouse's original design is examined first, and a reduction of transition length is examined afterwards.

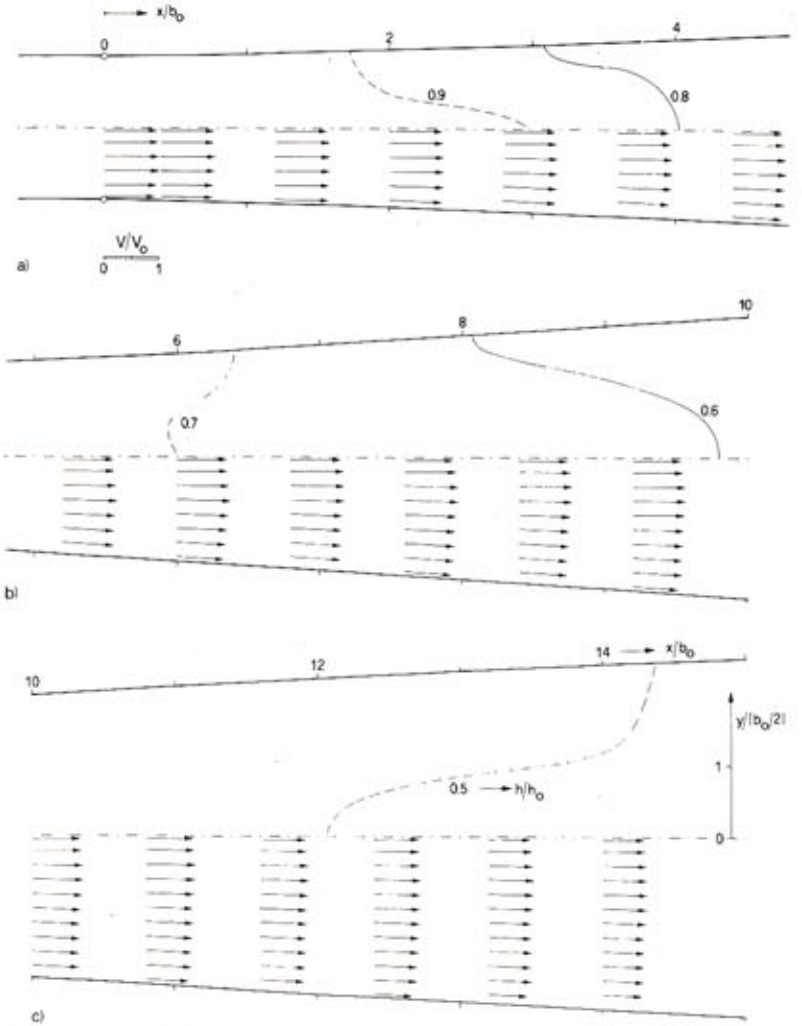

FIG. 5. Reversed Rouse Wall Curve for $F_D = 4$ (Run 9), Analogous to Fig. 2 Otherwise

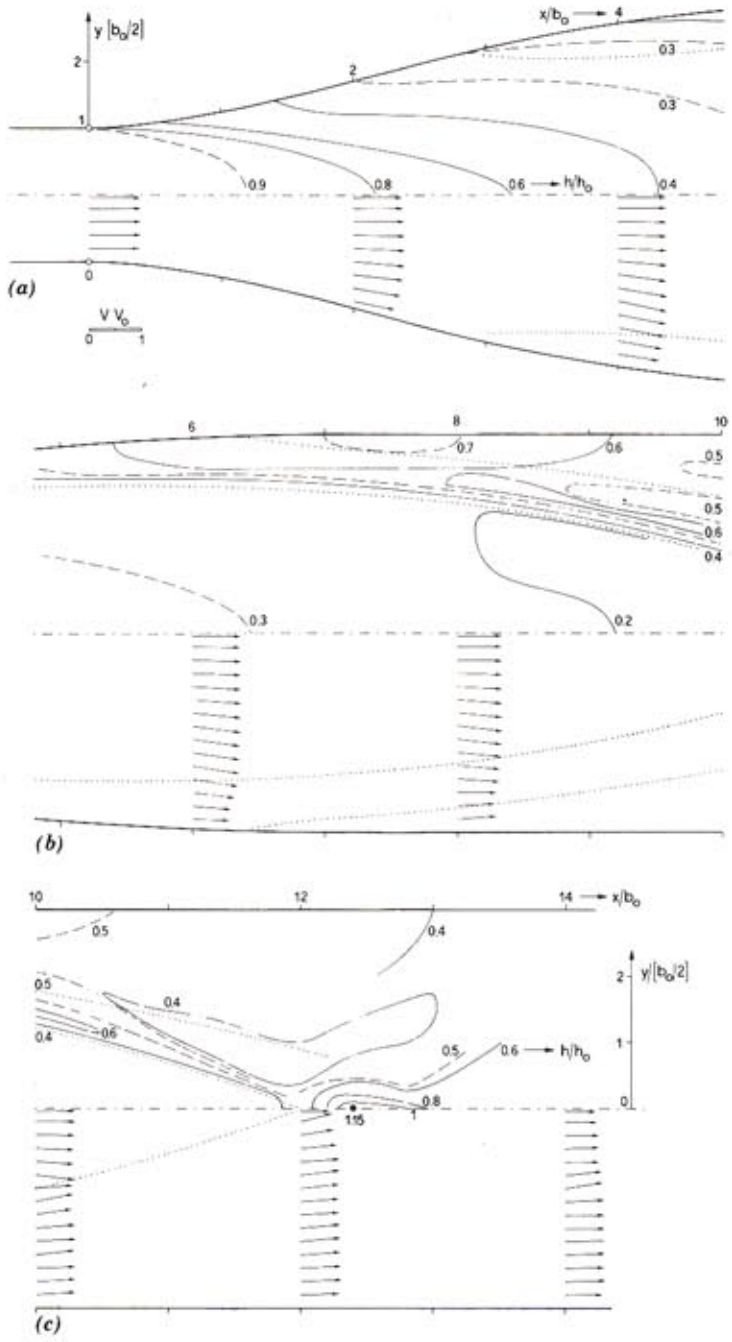

FIG. 6. Reversed Rouse Wall Curve for F_D = 1 and h_o = 96 mm; F_o = 4 (Run 43)

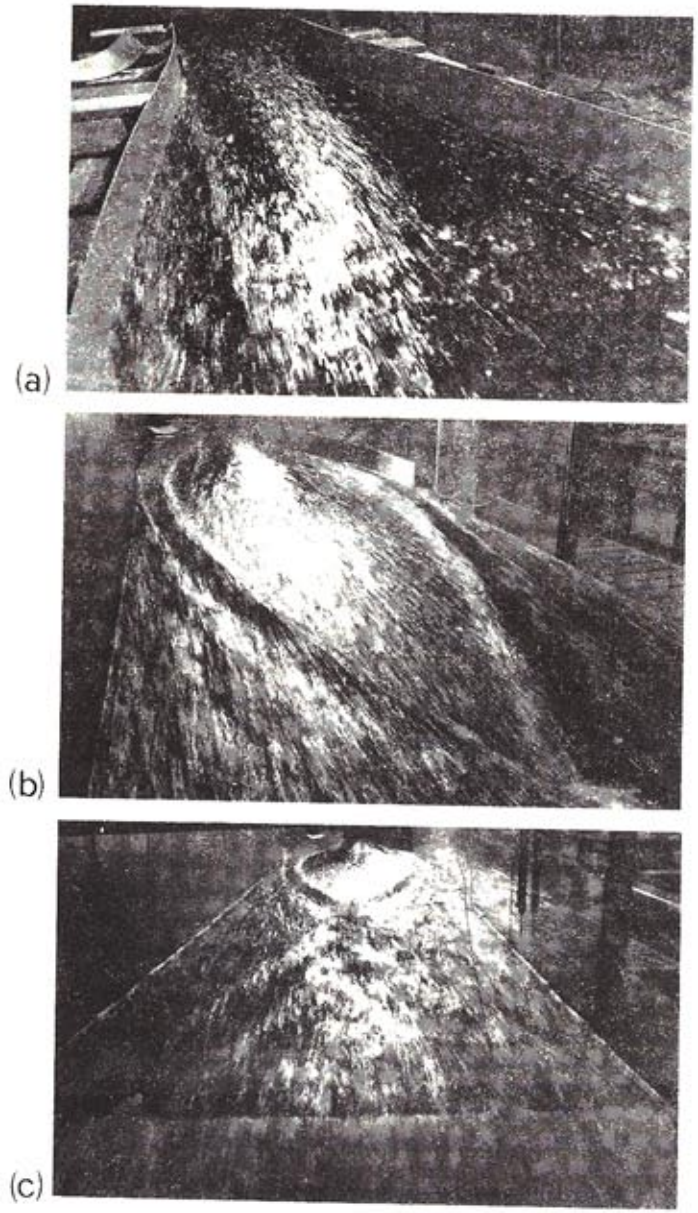

FIG. 7. Tailwater Views for Run 43, Rouse Reversed Wall Curve with F_o/F_D = 4

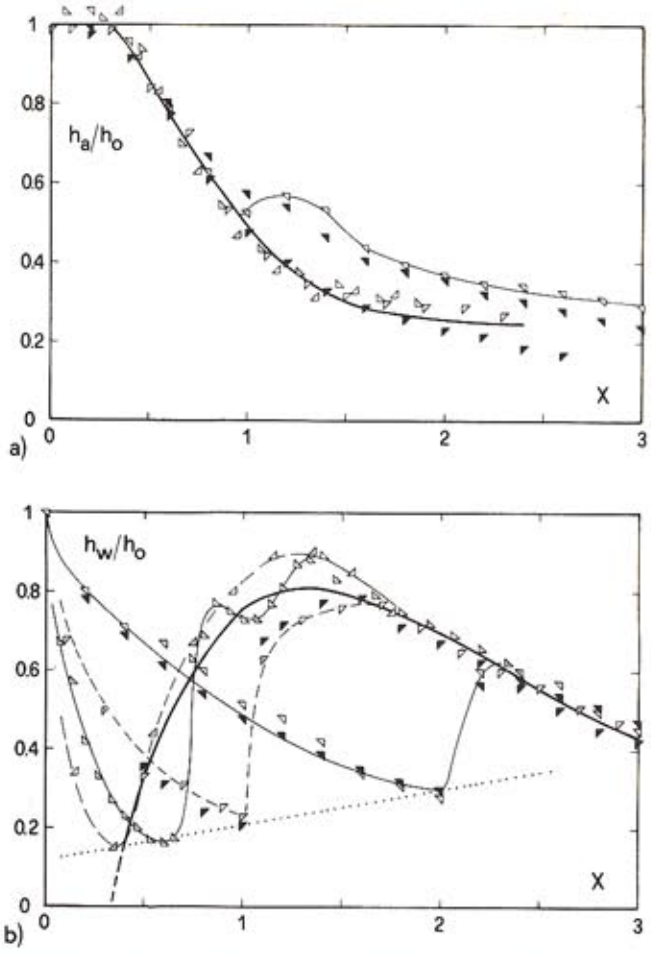

FIG. 8. Modified Rouse Curve for $F_D = 1$: (a) Axial Surface Profile $Y_a(X)$; and (b) Wall Surface Profile $Y_w(X)$ for F_0 = (▽)2, (▽)4, (△)6, (△)8; h_0 = 48 mm Light and h_0 = 96 mm Solid Symbols (—— = Abrupt Expansion Flow; .... = Lower Limit Curve)

Fig. 5 shows the analogous plot to Fig. 2, and only small differences may be noted. The flow in the expanding channel portion is again smooth for $F_0/F_D = 1$, but the tailwater reach cannot be seen, because the length of tailwater test channel (8 m) is much smaller than the transition length (15 m).

Next, a reversed Rouse wall curve was designed for $F_D = 1$; Fig. 6 shows the corresponding flow fields for $F_0 = 4$ ($F_0/F_D = 4$). The effect of expansion is now significant, mainly close to the expanding wall and in the axis reflection of shock ($x/b_0 \cong 12$). The maximum wall flow depth is 76% of h_0 and thus only slightly lower than as quoted for the abrupt expansion. The maximum axis flow depth is even 115% of h_0 as compared to 97% for the

abrupt expansion. The overall flow pattern is somewhat more uniform than for the corresponding abrupt and Rouse modified wall expansions, however.

Fig. 7 relates to the experiment shown in Fig. 6 and reveals only a small degree of perturbation within the expansion, but significant shock waves in the tailwater domain of wave crossing. Further downstream, those waves are considerably reduced and only a small amount of waviness continues in the tailwater channel.

The reversed expansion designed for $F_D = 1$ at an approach Froude number $F_0 = 2$ (run 44) revealed much less wave action and indicated acceptable flow conditions. Thus, the original design ($F_0/F_D = 1$) based on the reversed wall curve by Rouse et al. (1951) can be improved.

Experimental Results

Modified Rouse Wall Curve Expansion

The axial flow depth $h_a(x)$ and the wall flow depth $h_w(x)$ correspond to particular profiles of the free surface $h(x, y)$. Fig. 8(*a*) shows the axial surface profile $Y_a = h_a/h_0$ as a function of dimensionless length coordinate $X = (x/b_0)F_0^{-1}$ for the design Froude number $F_D = 1$. It is seen that all data lie on a single curve up to $X = 1$, where the first shock wave crosses the axis for $F_0 = 2$, and the curve has some local maximum. For $4 \leq F_0 \leq 8$, the data continue on a single curve up to the point where the respective shock also crosses the axis. Also included in Fig. 8(*a*), is a solid curve, showing the axial surface profile for $h_0 = 48$ mm of the abrupt expansion (Hager and Mazumder 1992). The modified Rouse wall curve and the abrupt expansion generate identical axial flow. The data pertaining to the approach flow depth $h_0 = 96$ mm follow essentially the same trend, except that wall friction is reduced for $X > 2$ and the curve is therefore slightly lower than for $h_0 = 48$ mm.

In Fig. 8(*b*) the wall surface profile $Y_w(X)$ is plotted with $Y_w = h_w/h_0$ and $X = x/(b_0F_0)$. Because the end of the modified Rouse curve is located at $L_t = 2.00$ m for all runs, the normalized transition length varies with F_0, and so do the wall profiles. However, a systematic trend may readily be seen, also as regards the minimum flow depth h_{wm}. The difference between maximum (index M) and minimum (index m) flow depths h_{wM} and h_{wm} increases with F_0, and so does the nonuniformity. The maximum flow depth, however, is larger than the corresponding value $Y_{wM} = 0.81$ for the abrupt expansion, because $Y_{wM} = 0.89$ ($F_0 = 6$) and $Y_{wM} = 0.91$ ($F_0 = 8$). As a result, the modified Rouse wall curve is a poorer design (as regards the necessary wall height) than the abrupt expansion. Table 2 shows that the location x_M of maximum wall depth is better centered in the Rouse modified wall curve than in the abrupt expansion (where $X_M = 1.33$).

Also, for $F_0 < 6$, the end of the modified Rouse curve is located downstream from the end of the corner separation curve as obtained for the abrupt expansion; whereas the modified Rouse wall curve is "overforced"

TABLE 2. Location x_M/b_0 of Maximum Wall Depth for Modified Rouse Wall Curve and Abrupt Expansion

F_0 (1)	2 (2)	4 (3)	6 (4)	8 (5)
Modified	6.2	6.4	8	10
Abrupt	2.65	5.3	8	10.6

for $F_0 = 8$. This might be the reason for secondary waves along the wall as shown in Fig. 8(*b*). Another feature of this plot is the similarity of $Y_w(X)$ for all values of F_0 beyond the location of maximum wall flow depth, and the superposition of the corresponding curve for the abrupt expansion. The data regarding $h_0 = 96$ mm follow almost perfectly those of $h_0 = 48$ mm, and no scale effect may be detected for both $F_0 = 2$ and 4.

Fig. 9 refers to the axial and wall velocity profiles V_a/V_0 and V_w/V_0 as functions of dimensionless distance X. Both distributions depend on the approach Froude number F_0 as well as on the approach flow depth h_0. As a result, the velocity distribution is governed by significant scale effects, and no generalized information may be given as it can for abrupt expansions. The data for V_w/V_0 and $F_0 = 2$ are not included, because they follow a different trend.

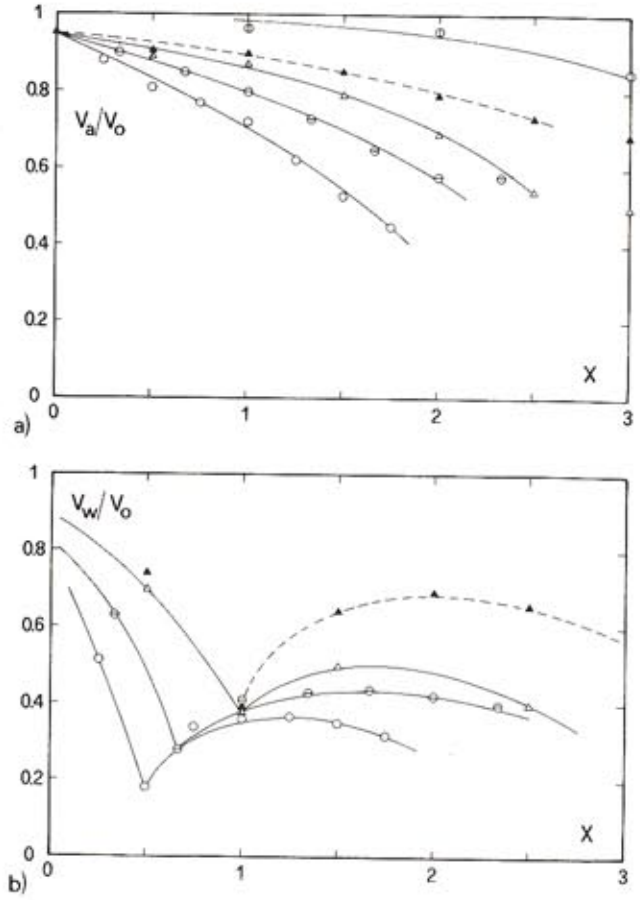

FIG. 9. Longitudinal Velocity Distributions as Function of X for $F_D = 1$: (*a*) Axial Velocity Ratio V_a/V_0; and (*b*) Wall Velocity Ratio V_w/V_0; F_0 = (⊕)2, (△)4, (⊖)6, (○)8 for $h_0 = 48$ mm, and F_0 = (▲)4 for $h_0 = 96$ mm

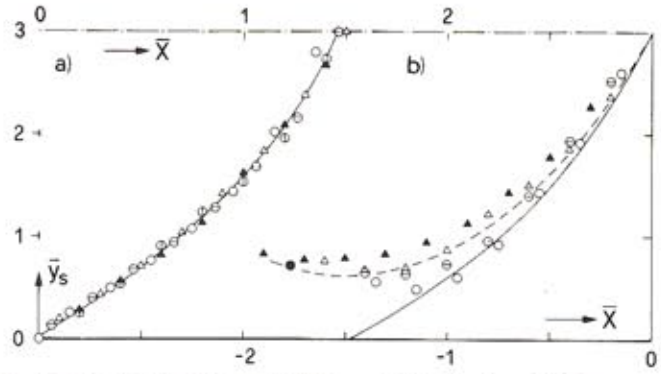

FIG. 10. Location of Shock Front $\bar{y}_s(\bar{X})$ for: (*a*) Modified; and (*b*) Reversed Rouse Wall Curves (Notation as in Fig. 9; —— = Eq. (1); ---- = Average Curve)

In Fig. 10(*a*), the location of the shock front is plotted as $\bar{y}_s(\bar{X})$. The coordinate $\bar{X} = (x - L_t)/(b_0F_0)$ has its origin at the end of the modified Rouse curve corresponding to $L_t = 2.0$ m and $\bar{y}_s = y_s/(b_0/2)$.

An almost perfect similarity occurs for $h_0 = 48$ mm. The data for $h_0 = 96$ mm and $F_0 = 4$ also collapse on the average curve

$$\bar{y}_s = (1 + \varepsilon)\tan(\varepsilon\bar{X}); \qquad \varepsilon = \frac{8}{9} \qquad \ldots\ldots\ldots\ldots\ldots\ldots\ldots\ldots\ldots\ldots (1)$$

The data for $h_0 = 96$ mm and $F_0 = 2$ deviate slightly again, however.

The standard deviation σ of the free-surface profile from the cross-sectional average $\bar{h}$ may be considered as a measure for free-surface uniformity. Fig. 11(*a*) shows σ both along the transition length $0 \le x/L_t \le 1$, and the tailwater reaches $\bar{X} = (\bar{x} - L_t)/(b_0F_0)$. Along the transition length, σ increases with the approach Froude number F_0. For $F_0 = 2$, σ remains below 0.1 but increases to a maximum value of $\sigma = 0.24$ for $F_0 = 4$. The data for $F_0 = 6$ and 8 follow the same trend and are much higher than for smaller F_0. In the tailwater channel, the data for $4 \le F_0 \le 8$ may be plotted together with the curve for the abrupt expansion when shifting the latter by $\Delta X = -0.6$; that is, to the point where the flow impinges the side walls. The curve for $F_0 = 2$ follows a different trend, with $\sigma \le 0.3$. Therefore, and this conclusion was also reached visually, flows with $F_0/F_D \ge 3$ are unacceptable in a modified Rouse curve expansion. Flows with a smaller Froude number ratio such as $F_0/F_D = 2$ to 2.5 may be considered acceptable.

Reversed Rouse Wall Curve Expansion

The axial surface profile $Y_a(X)$ is shown in Fig. 12(*a*) for the design curves $F_D = 1$ and 4. For $F_D = 1$ the data follow three different, distinct curves. All curves cross at $X \cong 0.7$. For $F_0 = 1$ and $F_0 = 2$ the difference of height is about $\Delta Y_a = 0.1$ for $X > 1.5$. The same difference of elevation occurs between the curves corresponding to $F_0 = 2$ and $F_0 = 4$. The data for $F_0 = 4$, 6, and 8 are located on the same full curve valid for the abrupt expansion. As a result, there is no difference between the abrupt and the reversed Rouse wall curve if $F_0/F_D \ge 3$ (see the following).

The wall surface profiles are shown in Fig. 12(*b*). Note how gradual the transition is for $F_0 = 1$ from $Y_w(0) = 1$ to $Y_w(3) = 0.3$ and $Y_a(3) = 0.35$.

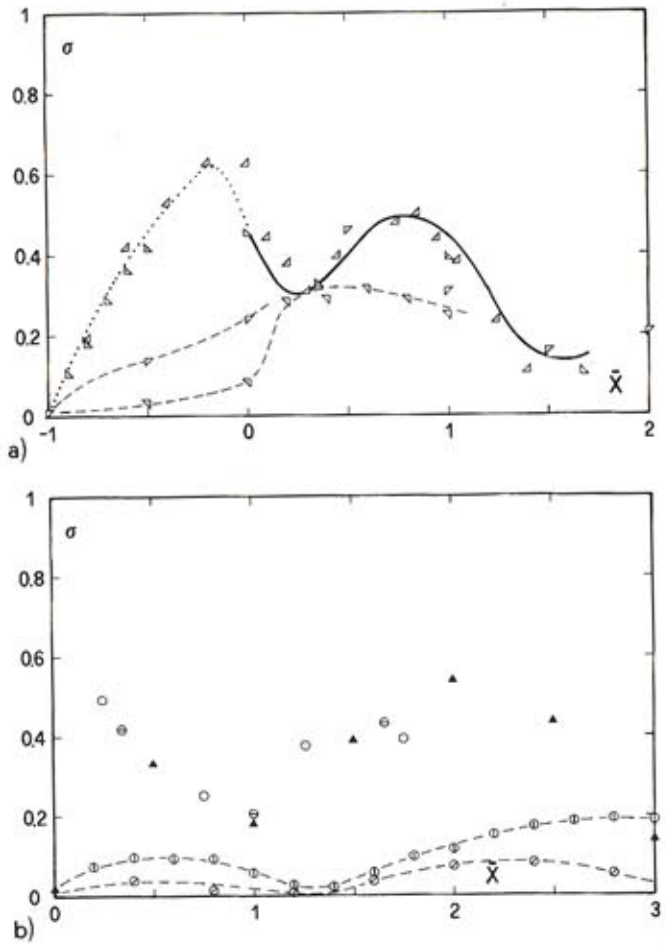

FIG. 11. Standard Deviation σ as Function of Dimensionless Distance $\bar{X}$ for: (a) Modified; and (b) Reversed Rouse Wall Curves (Notation as in Figs. 8 and 9; ---- = Curves for F_0 = 2 and 4; .... = Average Curve for F_0 = 6 and 8; —— = Abrupt Expansion)

For $F_0 = 2$, some standing waves occur, and $Y_a(3) = 0.25$ and $Y_w(3) = 0.42$ with an average of 0.33. For $F_0 = 4$ a wall minimum depth of $Y_w = 0.3$ occurs at $X = 0.6$, then the depth increases to a first maximum of $Y_{wM}(1.8) = 0.76$. Further downstream the data collapse with the curve for the abrupt expansion. For $F_0 = 6$ and 8, the minimum depth is lower and the maximum depth somewhat higher, but there is essentially also the trend as given by the abrupt expansion.

The axial velocity distribution V_a/V_0 (not shown) as a function of X depends strongly on the scale h_0 and on F_0, as does the velocity distribution in the modified Rouse wall curve. This effect is also attributed to wall friction—and scaling is impossible. To the lowest order of approximation, the axial velocity may also be considered constant for $X < 3$ and large values

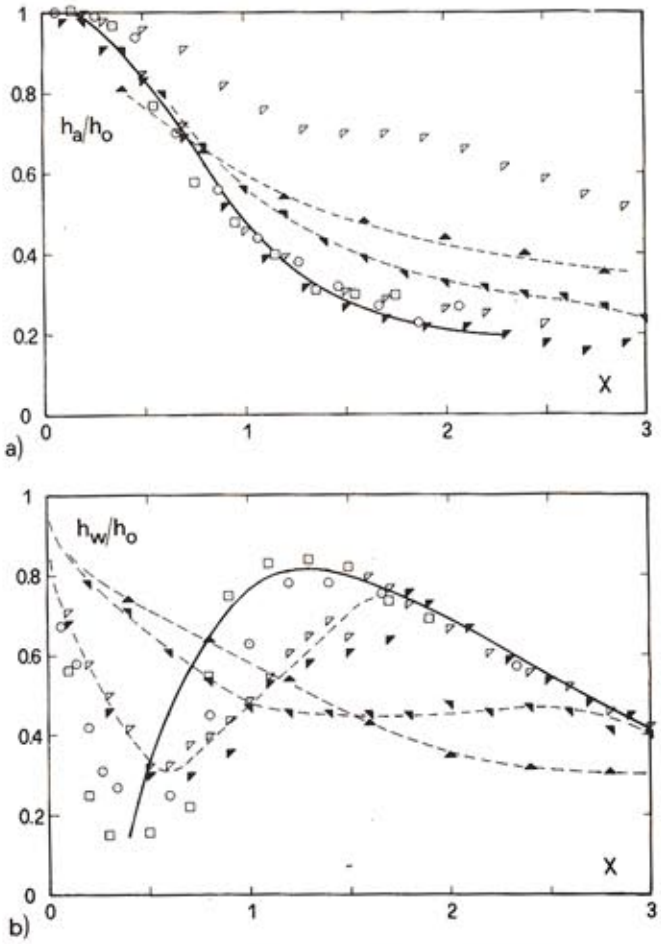

FIG. 12. Rouse Reversed Wall Curve: (a) Axial Surface Profile $Y_a(X)$; (b) Wall Surface Profile $Y_w(X)$ for F_D = 1 and F_0 = (▲)1, (◥)2, (◤)4 for h_0 = 96 mm; and (▽)4, (○)6, and (□)8 for h_0 = 48 mm; F_D = 4; F_0 = (▽)4 [---- = Average Curves; —— = Curve for Abrupt Expansion (Hager and Mazumder 1992)]

of h_0. The wall velocity distribution follows practically the curves of the modified Rouse curves [Fig. 9(*b*)], except that the first minimum is not so abrupt. After the initial drop of velocity in the domain of transition, the wall velocity remains approximately constant.

The shock curve follows a more difficult path than that for the modified Rouse curve. In the latter, there is a definite origin at the end of transition $x = L_t$; whereas the reversed transition is smooth and the geometry is not scaled by F_0. Also, for low Froude numbers the main shock curve is followed by a secondary oscillation, which was absent for $F_0 > 6$. The location of shock front $\bar{y}_s(\bar{X})$, where $\bar{X} = (x - x_0)/(b_0 F_0)$, is plotted in Fig. 10(*b*), with the origin $\bar{X} = 0$, where the shock crosses the channel axis. The computational origin x_0 of shock generation may be expressed as $x_0/b_0 = 8 + F_0$.

The standard deviation σ of the transverse surface profiles $h(y)$ at a distinct location x relative to the average $\bar{h}(x)$ is plotted in Fig. 11(b); σ-values of almost zero are seen for $F_0 = 1$ and 2, but a much more nonuniform pattern occurs for $F_0/F_D \geq 4$. Again, the wall geometry is overforced when the ratio F_0/F_D is too large.

Design of Expansion

A particular experiment was conducted in which the optimum approach Froude number F_0 for a given design Froude number F_D of the Rouse expansion was determined for the expansion ratio $\beta = 3$. Several parameters were recorded, including the maximum wall flow depth h_e in the primary shock wave, the maximum center flow depth h_M at the crossing of shock waves, the corresponding wall flow depth h_{w1}, the location x_M, and the maximum wall flow depth h_{w2} of the secondary cross wave (Fig. 13).

All depths normalized by h_0 start at some fictitious value 0.4 for $F_0/F_D \to 1$ [Fig. 14(a)]. The increase of the depth h_e/h_0 and h_{w1}/h_0 is relatively small, and it levels off for large F_0/F_D. The increase of h_{w2}/h_0 is larger and could only be recorded until $F_0/F_D = 3.7$ due to the limited channel length. The curve for the maximum flow depth h_M/h_0 has a maximum of 1.7 for

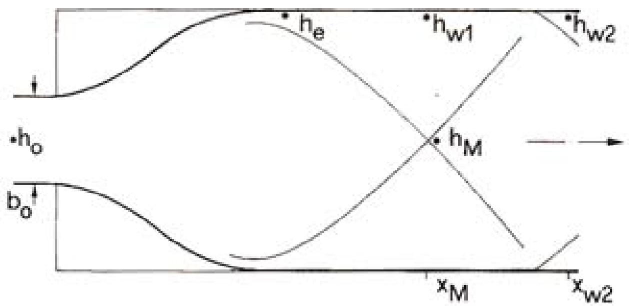

FIG. 13. Definition of Flow Geometry in Rouse Reversed Expansion

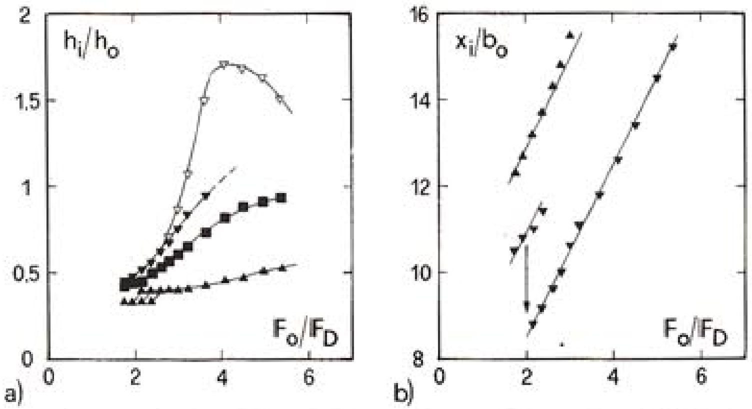

FIG. 14. Characteristics of Flow in Rouse Reversed Expansion: (a) Relative Flow Depths (▲) h_{w1}/h_0, (■) h_e/h_0; (▼) h_{w2}/h_0; (▽) h_M/h_0; (b) Relative Locations (▼) x_M/b_0; (▲) x_{w2}/b_0 as Functions of F_0/F_D

$F_0/F_D = 4$. Increasing F_0/F_D beyond 4 drops the maximum center flow depth. Another interesting feature occurs with h_{w1}/h_0: two values occur for low $F_0/F_D < 2.5$ due to the modular surface pattern.

Based on these and previous experiments, as well as on extended additional observations, one may conclude that the original Rouse reversed wall curve is too long for practical purposes. The recommended design Froude number F_D for the reversed wall curve from actually $F_0/F_D = 1$ may be increased to $F_0/F_D = 2.5$. From Fig. 14(a), the wave heights h_M and h_{w2} are then still equal, the maximum center flow depth is still small, and the effect of wall curvature on the shock pattern is not excessive. The following design relations hold [Fig. 14(a)]: (1) $h_e = 0.52h_0$; (2) $h_M = h_{w2} = 0.6h_0$; and (3) $h_{w1} = 0.4h_0$. From Fig. 14(b) the locations of maximum wall depths are $x_{w1} = 7.5b_0$ and $x_{w2} = 14b_0$; the maximum center depth occurs at $x_M = 9.5b_0$. For all discharges other than the design discharge, which is normally the discharge with the maximum approach Froude number F_0, the design parameters can be read from Fig. 14. The procedure can also be extended to other expansion ratios $\beta = b_2/b_0$, because this will hold true correspondingly.

Conclusions

Based on an extended experimental program, the flow pattern in expansions with modified and reversed Rouse wall geometries was determined for supercritical approach flow. Compared to the flow in an abrupt expansion, the modified wall geometry does not improve the flow and may not be recommended. However, the reversed Rouse wall geometry yields satisfactory results even when shortened by a factor of 2.5 as compared to the original Rouse design. This reduction is significant because the length of transition structure obtains only 40% with a comparable overall flow pattern.

Apart from this design recommendation, the present analysis reveals partial similarity in a supercritical 2D free-surface flow. Whereas the free surface may be represented by a coordinate system distorted by F_0^{-1} in the streamwise direction, the velocity field is governed by a significant viscous effect; and simple scaling is impossible. Additional information such as the geometry of shock front, the distribution of standard deviation, and the location of wave peaks are also given to yield a quite complete flow description in chute expansions.

Acknowledgments

The writers are grateful to Prof. R. Sinniger, Director of the Institute of Hydraulics and Energy of the Swiss Federal Institute of Technology, in Lausanne (EPFL), who supported the present study during the sabbatical leave of the first writer.

Appendix I. Rouse's Wall Curves

Based on a computational model, Rouse et al. (1951) determined the boundary curve $y_e(x)$ enclosing some 90% of discharge in an abrupt expansion as

$$\frac{y_e}{b_0} = \frac{1}{2}(1 + X^{3/2}) \qquad (2)$$

Further, the so-called modified Rouse wall curve $y_b(x)$ was defined as

$$\frac{y_b}{b_0} = \frac{1}{2}\left(1 + \frac{1}{4}X^{3/2}\right) \quad \ldots\ldots (3)$$

The rate of expansion is thus much reduced to the "natural" expansion flow.

The Rouse reversed wall curve comprises the modified portion up to the point of tangency $0 < x < L_p$ and a backward curved downstream portion for $L_p < x < L_t$ (Fig. 1). The lengths obtain approximately for $1 < \beta \leq 5$

$$\frac{L_p}{b_0 F_0} = 0.7\beta \quad \ldots\ldots (4)$$

$$\frac{L_t}{b_0 F_0} = 1 + 3.25(\beta - 1) \quad \ldots\ldots (5)$$

With $X_B = (x - L_p)/(L_t - L_p)$ and $Y_B = (y - y_p)/(\beta b_0/2 - y_p)$, where $y_p = y_b(x = L_p)$ according to (3) and (4), the transition curve may be approximated from Rouse et al. (1951) as

$$Y_B = \sin(90°X_B) \quad \ldots\ldots (6)$$

In the present experiments, the Rouse reversed wall curves were taken directly from Rouse et al.'s plot.

Appendix II. References

Chow, V. T. (1959). *Open channel hydraulics*. MacGraw-Hill Book Co., Inc., New York, N.Y.

Hager, W. H. (1992). "Spillways. Shockwaves and air entrainment." *ICOLD Bulletin 81*, Commission Internationale des Grands Barrages, Paris, France.

Hager, W. H., and Mazumder, S. K. (1992). "Supercritical flow at abrupt expansions." *Proc., Inst. of Civ. Engrs.—Water, Maritime, and Energy*, London, England, 96, 153–166.

Rouse, H., Bhootha, B. V., and Hsu, E. Y. (1951). "Design of channel expansions." *Trans.*, ASCE, 116, 1369–1385.

Appendix III. Notation

The following symbols are used in this paper:

b = channel width;
F = Froude number;
g = gravitational acceleration;
h = flow depth;
$\bar{h}$ = average cross-sectional flow depth;
h_e = flow depth at primary shock wave;
L_t = transition length;
V = magnitude of velocity;
X = $x/(b_0F_0)$ normalized x-coordinate;
$\tilde{X}$ = shifted X-coordinate;
X_t = X-coordinate in transition reach;
x = longitudinal coordinate;
Y = h/h_0 normalized flow depth;

y = transverse coordinate;
y_s = shock coordinate;
$\tilde{y}_s$ = $y_s/(b_0/2)$ normalized shock coordinate;
β = width ratio;
ε = parameter; and
σ = standard deviation.

Subscripts

a = axial;
D = design;
e = expansion;
M = maximum;
m = minimum;
o = approach;
p = point of tangency;
w = wall;
0 = origin of shock; and
2 = tailwater.